

# RATE CONTROL SYSTEM FOR SOUNDING ROCKETS

**Josef Ettl, Johann Pfänder**

German Aerospace Center (DLR),  
D-82234 Wessling, Germany

e-mail:

josef.ettl@dlr.de

johann.pfaender@dlr.de

## 1. ABSTRACT

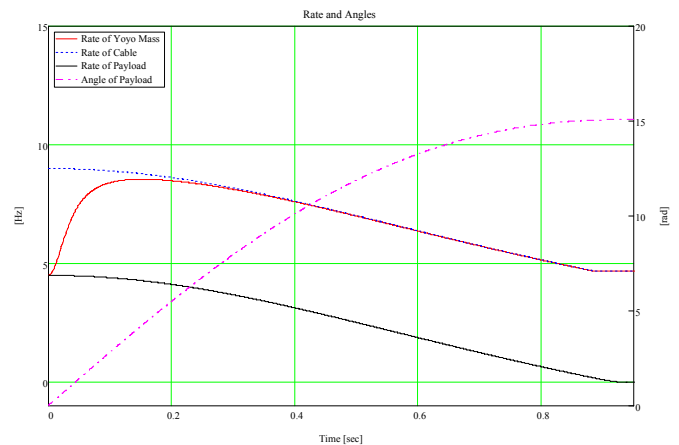
DLR/Moraba has a long history in the development of Rate Control Systems (RCS) which have been flown for several programs for research in weightlessness in Europe and Brazil. They had been used in various European  $\mu$ G programs such as MAXUS, MASER and TEXUS. Moraba has now developed a RCS for 14 inch payloads. This RCS uses a standard interface and can be easily joined to a REXUS service module. This combination (RCS and REXUS service system) came into operation for the MAPHEUS maiden flight.

MAPHEUS (Materialphysikalisches Experiment unter Schwerelosigkeit) is an internal project of the DLR. The payload for this project, including the service systems and 4 experiments, flew on a Nike/improved Orion two stage motor which took the payload to an altitude of about 140.8 km, providing a period of weightlessness of more than 187 seconds.

To achieve conditions of weightlessness above the atmosphere a RCS system is indispensable. The aim of the RCS is to reduce the angular rates of the payload significantly above the atmosphere in order to minimize the centrifugal accelerations to a level lower than  $10 \mu$ g. This article describes the principle of a rate control system. It provides an insight into the interaction between the control loop, payload and actuators.

## 2. INTRODUCTION

Many sounding rockets, constructed for ballistic flights, build up a spin around the roll axis to stabilize the flight vector during the ascent phase. The final spin frequency depends on the type of rocket. Spin rates in the range of several Hz are obtained. The spin rate must be reduced by a yo-yo system. The dimension of the yo-yo system depends on the inertia of the roll axis and the diameter of the payload. The following graph shows an example of a de-spin procedure.



Graph 1: Yo-Yo procedure

The basic task of the rate control system is to provide angular rate control (nominally zero angular rates) for sounding rocket microgravity payloads, thereby reducing the centrifugal accelerations to insignificant levels. The RCS can remove residual rates after payload separation and compensate for external or self induced torques but it can not compensate for linear accelerations such as those caused by drag.

The rate control system can be considered as three essentially independent control loops, one for each of the body fixed roll, pitch and yaw axes. A control loop comprises the sensor or sensors, the control processor, the torquers and the payload physical characteristics. The classical control schematic diagram for one axis is shown below.

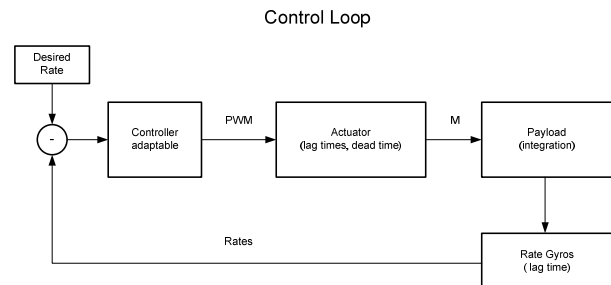
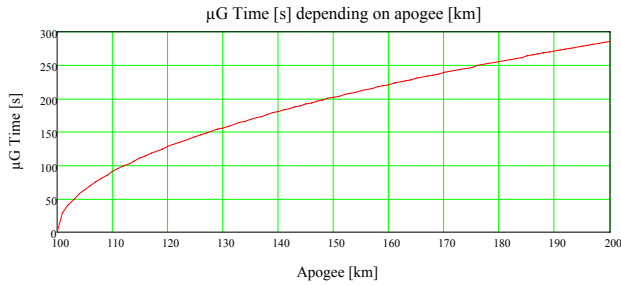


Figure 1: Control loop

After the de-spin activation, there will be a residual rate in all axes. These rates must be decreased by a RCS system in order to achieve  $\mu\text{G}$  conditions above 100 km altitude. The following graph shows the calculated achievable  $\mu\text{G}$  time depending on the apogee of the rocket.



**Graph 2:**  $\mu\text{G}$  period depending on apogee

### 3. RCS- SYSTEM DESCRIPTION

#### 3.1. Concept

The RCS system is a control system which shall reduce the rates in all axes independently. The RCS system is based on a cold gas system comprising a gas tank, regulators, solenoid valves and nozzles. Dry nitrogen is often used as a medium to generate the necessary thrusts for the reduction of any angular rates. For large payloads it is useful to implement a dual stage RCS system in order to reduce the angular movement with two different thrust levels in coarse and fine mode. The following schematic explains the principle of a single stage RCS system.

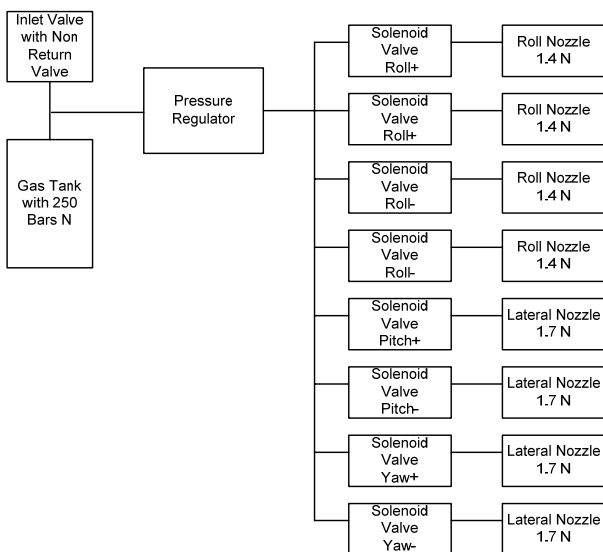


**Figure 2:** Block diagram for the RCS

The solenoid valves are controlled by a flight computer which also reads the rate sensors to receive a feed back from the angular rates. As the nozzles show a different behaviour on ground and in space, and as the final inertias of the payload often can not be determined exactly, it is a big advantage to implement an adaptive control algorithm, also to use this algorithm for different payload sizes in different projects.

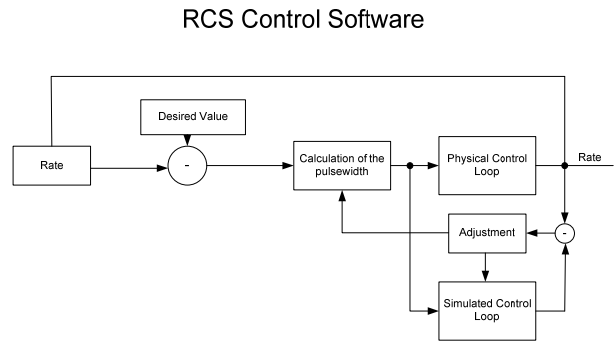


**Figure 3:** RCS control software

In principle there are two different philosophies to control the angular rates of a payload, designed for weightlessness, during the  $\mu\text{G}$  phase. The first philosophy is to reduce the rates and the resulting centrifugal accelerations as fast as possible in order to increase the quality and duration of weightlessness. This includes the disadvantage that the correction pulses degrade the weightless environment. The other philosophy is to control very smoothly and softly the angular rates to minimize the levels of disturbances.

It does not violate the  $1 \cdot 10^{-4}\text{G}$  limits, but it allows a worse quality of weightlessness for a longer period.

During the first acquisition, when the residual rates after the activation of the yo-yo system have been reduced, first the roll rate is decreased to minimize the cross coupling between the lateral axes. After the first acquisition a tolerance band of acceptable rates is established to minimize the number of control pulses. The amplitude of this band depends on the distance of the experiments from the centre of gravity and the desired weightlessness level.

#### 3.2. Actuators

The actuators comprise a combination of valves and nozzles. This combination generates thrust pulses which allow a pulse width modulation. The valves control the throughput of gas through the nozzles.

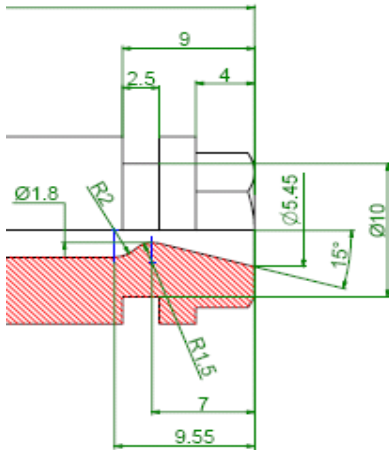
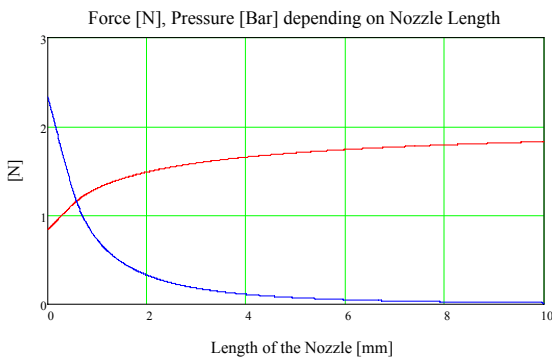
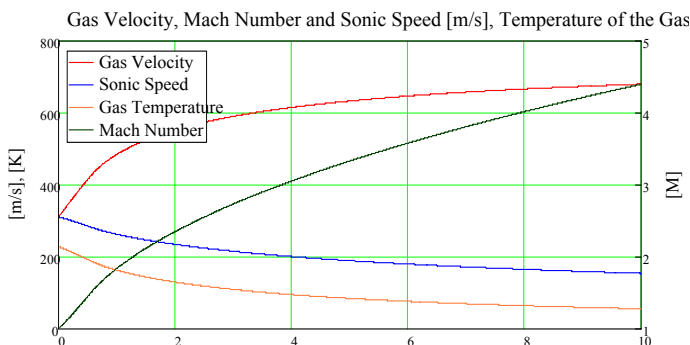


**Figure 4:** Schematic of a nozzle



**Graph 3:** Force and pressure along the nozzle axis

The graphic above shows a characteristic of an expansion nozzle. The pressure and the produced thrust depend on the length of the nozzle, input pressure and the diameter of the throat. At a length of about 8 mm no significant increases of the thrust are possible. The pressure within the nozzle decreases from about 2.3 Bar at the nozzle throat to almost 0 Bar at the end of the nozzle in space. The input pressure at the nozzle input is 4 Bar. The thrust of the nozzle is limited to a value of about 1.3 N at an atmosphere of 1 Bar instead of 1.8 N in space. The nozzle expands and accelerates the gas to a velocity of almost 700 m/sec which means 4 Mach at



**Graph 4:** Speed and temperature

a nozzle length of 8 mm. In parallel there are significant drops of the gas temperature and sonic speed.

### 3.3. Control Algorithm

The control algorithm is based on an adaptive control mechanism. The control algorithm adjusts itself to the characteristics of the control loop. Therefore variations and uncertainties of some loop parameters like thrust, moment arm, inertia, environmental pressure, etc are compensated by the flexible control algorithm. Furthermore, the control algorithm doesn't have to be changed from project to project.

### 3.4. Rate Sensors

The sensors are used to provide the feedback of the control loop. There are different types of sensors available. The main categories are electro-mechanical, MEMS and fibre optic sensors. Independent of the kind of sensors it is important to use sensors with the adequate output frequency and accuracy. The quality of the control loop depends mainly on the quality of the sensors. Sensors without any moving parts like MEMS or fibre optic sensors have several advantages. Their handling is easy and the degradation of the sensors by time is smaller than with electro-mechanical sensors.

### 3.5. Single Stage RCS System as example

The following image shows a single stage RCS system which can normally be used for small payloads.



**Figure 5:** Image of the MAPHEUS RCS

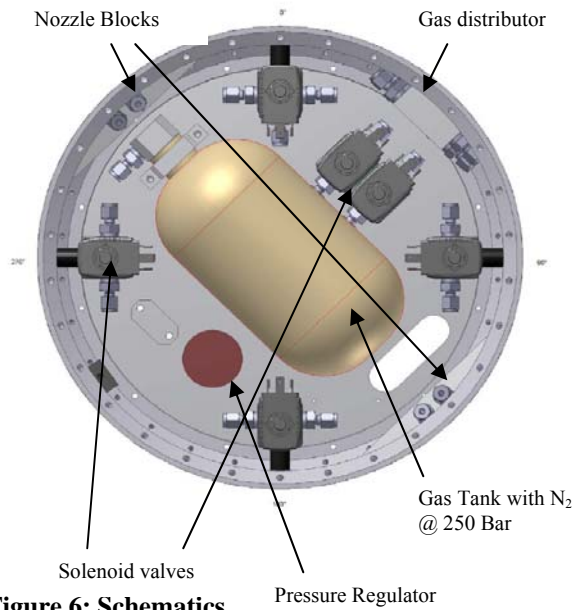


**Figure 6: Schematics**

This RCS system was designed for a 14 inch payload which flew on a Nike/improved Orion motor combination. The RCS system is adapted to payloads with inertia in the roll axis of up to 5 kgm<sup>2</sup> and an inertia in the lateral axes of up to 200 kgm<sup>2</sup>.

#### 4. DISTURBANCES

We can determine three different main sources of disturbances during the phase of weightlessness for parabolic flights. The first source is the acceleration resulting from the aerodynamic drag, depending on the density of the air, the velocity of the payload, the effective area, the shape of the payload and the angle of attack. Calculations and results of preceding projects showed that above 100 km altitude  $\mu$ G levels better than  $1 \cdot 10^{-4}$  g can be achieved.

The formula for the air drag is:

$$a = 0.5 \cdot c_d \cdot A \cdot D \cdot V^2 \cdot \sin(\alpha) [m/sec^2]$$

$c_d$  = air drag coefficient

A=effected area

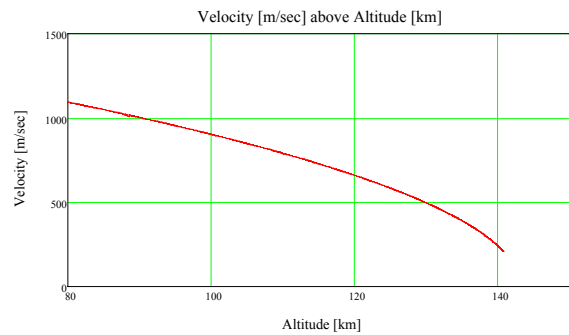
D=density

$\alpha$ =angle of attack

V = payload velocity

It is obvious from the formula that the velocity and the density have a big influence on the drag and therefore on the quality of the weightlessness. The next graph

shows the velocity of the payload above the altitude of 80 km.



**Graph 5: Velocity over altitude**

After the ejection of the nose cone and the separation from the second stage motor the payload has roughly the shape of a cylinder with a length of 2.76 m and a diameter of 0.356 m.

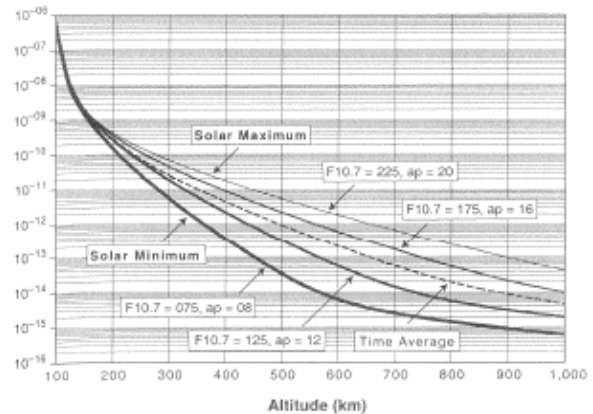


**Figure 7: Air density over altitude**

On the base of the preceding information one can calculate the g-level for the altitude of 100 km and at the apogee of about 140.8 km and find that the g-level will decrease from  $1 \cdot 10^{-4}$  g at 100 km altitude to about  $2 \cdot 10^{-6}$  g at the apogee.

The second source for disturbances is the acceleration based on the angular rate of the payload. It depends mainly on the dimensions and the angular movement of the payload. The acceleration can be calculated by the formula:

$$a = \omega^2 \cdot r [m/sec^2]$$

$\omega$  = rate

r = distance from centre of gravity

Assuming a rate of 0.4 deg/sec and a maximum distance of 1.4 m from the centre of gravity of an experiment, a disturbance of about 4  $\mu$ g can be calculated.

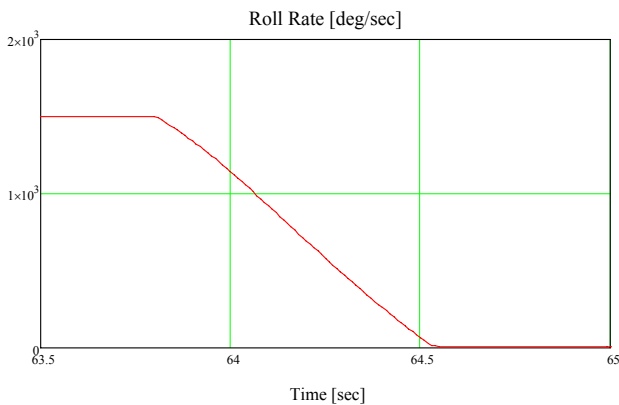
The last main source of disturbances during the phase of weightlessness is the payload itself, in particular the different experiments with their moving masses, their rotating elements, switching of valves and the control pulses of the gas system. A control pulse of the RCS system generates a disturbance of less than 1 mG for a duration of 0.5 sec. In order to avoid these shocks a tolerance band of rates for each axis is established. These tolerance bands allow disturbances in the order of  $1 \cdot 10^{-5}$  g, resulting from the centrifugal acceleration.

## 5. FLIGHT DATA

The following flight data were obtained from the MAPHEUS 01 maiden flight. The physical values like acceleration and rates were measured by the service module. The resolution for the accelerometer sensors is  $1 \mu\text{G}$  while the resolution for the rate sensors is  $0.03 \text{ deg/sec}$ . The absolute accuracy of the acceleration sensors after post-processing is in the range of about  $\pm 5 \mu\text{G}$  and of the rate sensor  $\pm 0.03 \text{ deg/sec}$ .

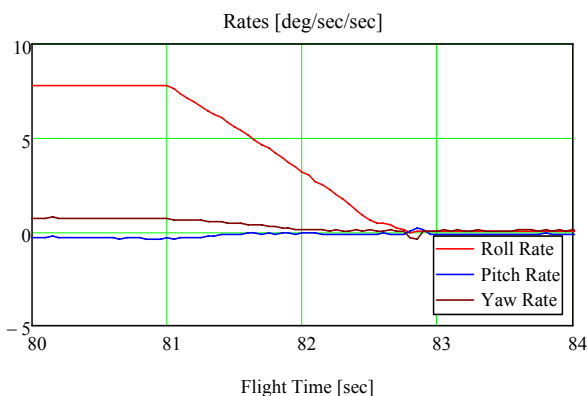
### 5.1. RCS Date

The following graph shows the reduction of the roll rates by the yo-yo system. This procedure takes only 0.9 sec and reduces the spin frequency from 4.5 Hz to almost 0 Hz

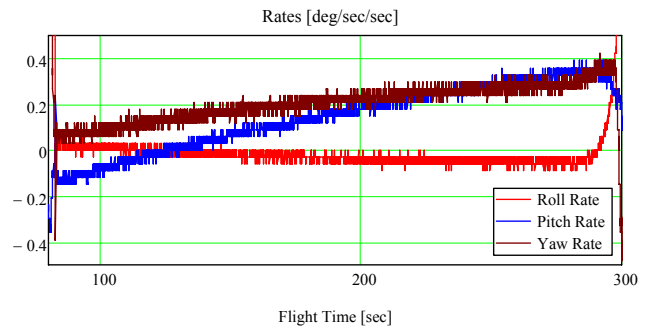


**Graph 6:** Roll rate during de-spin

The next graph illustrates the first acquisition of the RCS system where the residual rates in all axes are reduced to less than  $0.2 \text{ deg/sec}$  within 1.7 sec.

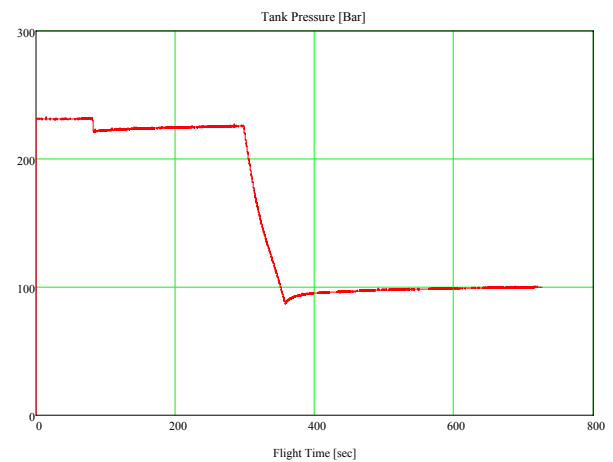


**Graph 7:** Rate at the initial acquisition

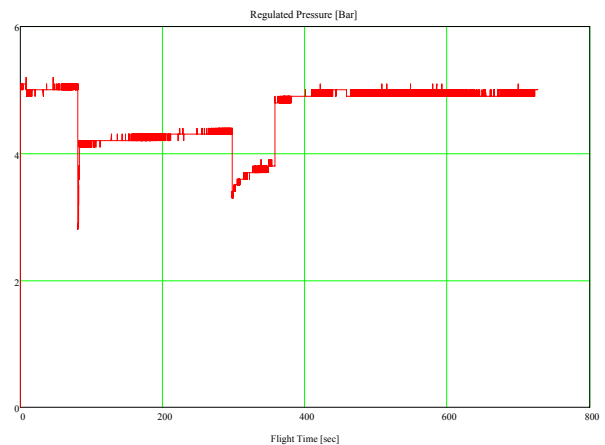


**Graph 8:** Rates during the  $\mu\text{G}$  phase

In graph 8 the rates during the  $\mu\text{G}$  phase are visible. It is obvious that during this phase, no control pulses were necessary.



**Graph 9:** Tank pressure



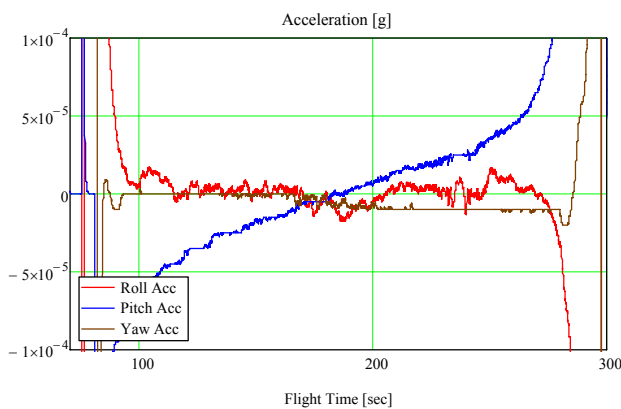
**Graph 10:** Regulated pressure

During the control phase of the flight only 10 % of the gas was consumed. About 50% of the gas was used to bring the payload into the spin mode around the roll axis after the  $\mu\text{G}$  phase to support the flat spin.

2. Space Mission, Analysis and Design, Third Edition from James R. Wertz and Wiley J. Larson

## 5.2. Acceleration

The following graph shows the accelerations during the  $\mu\text{g}$  phase. Although the roll and the yaw axes show a very stable acceleration during the  $\mu\text{G}$  phase, there is a higher and alternating 'g' level visible in the pitch axis. The reason for this is the higher angle of attack in this axis and the unfavourable direction of the measurement axis regarding the flight vector. The period of  $\mu\text{G}$  conditions ( $< 1 \cdot 10^{-4}$  g) lasted longer than 187 seconds during the MAPHEUS 01 flight



**Graph 11:** Acceleration during the  $\mu\text{G}$  phase

## 6. SUMMARY

The MAPHEUS maiden flight achieved a  $\mu\text{G}$  environment for more than 3 minutes. The resulting data showed that the REXUS service module, the yo-yo and the RCS system supported the establishment of a  $\mu\text{G}$  environment very well. The single stage RCS system is now qualified for further applications. The main characteristics of the system, like thrust levels and gas consumption, are very close to the theoretical values. The handling of the gas system had shown that it is a highly integrated and compact system and especially the loss of gas on the high pressure side is negligible.

I would like to thank all persons who participated in this successful mission.

## 7. REFERENCES

1. MP01-09-05-04 MAPHEUS-01 Flight Requirement Plan from Andreas Stamminger, 2009